Modeling inter-annual and spatial variability of ice cover in a temperate lake with complex morphology

Caramatti Irene (Orcid ID: 0000-0002-9663-0175)

Modeling inter-annual and spatial variability of ice cover in a temperate lake with complex morphology

Irene Caramatti [1], Frank Peeters [1], David Hamilton[2], Hilmar Hofmann [1]

[1] University of Konstanz, Konstanz, Germany

[2] Australian Rivers Institute, Griffith University, Brisbane, Queensland, Australia

Irene Caramatti

Mail address: irene.caramatti@uni-konstanz.de

Frank Peeters

Mail address: Frank.Peeters@uni-konstanz.de

David Hamilton

Mail address: david.p.hamilton@griffith.edu.au

Hilmar Hofmann

Mail address: hilmar.hofmann@uni-konstanz.de

This article has been accepted for publication and undergone full peer review but has not been through the copyediting, typesetting, pagination and proofreading process which may lead to differences between this version and the Version of Record. Please cite this article as doi: 10.1002/hyp.13618

Acknowledgments

We thank Chris Dallimore and Chris O'Neil from Hydronumerics for their help and support with the model setting. We are grateful to Orlane Anneville (French National Institute for Agricultural Research) who provided expertise that greatly assisted the research. We acknowledge the Water Police for the ice data, MeteoSchweiz for the COSMO wind data and the German Weather Service (DWD) for the meteorological data. The field data (CTD profiles, inflows, outflows, water level) was provided by the Landesanstalt fuer Umwelt Baden-Wuerttemberg (LUBW), the BOWIS- Water information system of Lake Constance from the International Commission for water protection of Lake Constance (IGKB), the Hydrographic Service Vorarlberg (VA), and the Swiss Federal Office for the Environment (BAFU). We also would like to thank Leon Walther that helped with the translation of the ice reports of the Water Police.

This study was financially supported by the German Research Foundation (DFG) within the framework of the RTG R3 (Research Training Group – Responses to biotic and abiotic changes, Resilience and Reversibility of lake ecosystems), grant number 298726046/GRK2272/A4.

Modeling inter-annual and spatial variability of ice cover

Key words: numerical modeling, AEM3D, hydrodynamic, lake, ice cover, thin ice

Abstract

The formation of ice cover on lakes alters heat and energy transfer with the water column. The fraction of surface area covered by ice and the timing of ice-on and ice-off therefore affects hydrodynamics and the seasonal development of stratification and related ecosystem processes. Multi-year model simulations of temperate lake ecosystems that freeze partially or completely therefore require simulation of the formation and duration of ice cover. Here we present a multi-year hydrodynamic simulation of an alpine lake with complex morphology (Lower Lake Constance, LLC) using the three-dimensional (3D) model AEM3D over a period of 9 years. LLC is subdivided into three basins (Gnadensee, Zeller See and Rheinsee) which differ in depth, morphological features, hydrodynamic conditions, and ice cover phenology and thickness. Model results were validated with field observations and additional information on ice cover derived from a citizen science approach using information from social media. The model reproduced the occurrence of thin ice as well as its inter-annual variability and differentiated the frequency and extent of ice cover between the three sub-basins. It captured that full ice cover occurs almost each winter in Gnadensee, but only rarely in Zeller See and Rheinsee. The results indicate that the 3D model AEM3D is suitable for simulating long-term dynamics of thin ice cover in lakes with complex morphology and inter-annual changes in spatially heterogeneous ice cover.

Introduction

The presence, formation and duration of ice cover substantially affects mixing conditions and biogeochemistry of lakes during winter months (Hampton et al., 2017). Furthermore, timing and duration of ice cover have a substantial influence on seasonal plankton succession, on the duration of the growing season and oxygen depletion, and thus also on the occurrence of anoxia in deep water.

During ice cover, the water column hydrodynamics are significantly modified by lack of wind stress at the water surface, which decreases vertical mixing (Fujisaki, Wang, Bai, Leshkevich, & Lofgren, 2013). Ice and snow cover limits penetration of solar radiation into the water column (Gerbush, Kristovich, & Laird, 2008) and reduces the exchange of water, heat and gases (Loose, McGillis, Schlosser, Perovich, & Takahashi, 2009). However, clear ice conditions can be favorable for winter phytoplankton blooms, since the water column is inversely thermally stratified and vertical mixing is limited (Vanderploeg, Bolsenga, Fahnenstiel, Liebig, & Gardner, 1992; Lizotte, Sharp, & Priscu, 1996; Arrigo et al., 2012; Hampton et al., 2017).

Climate change is likely to affect lake ice cover due to a predicted increase of air temperature in winter. This will cause a reduction in the occurrence of ice cover related to a delay in ice-on, earlier ice-off and thinner ice cover (Magnuson et al., 2000; Hodgkins, James, & Huntington, 2002; Austin & Colman, 2008; Dessai, Hulme, Lempert, & Pielke Jr, 2009; Mishra, Cherkauer, & Bowling, 2011; Hamilton, Magee, Wu, & Kratz, 2018).

Ice cover in European alpine lakes as well as in lakes worldwide (Magnuson et al., 2000; Weyhenmeyer, Westöö, & Willén, 2007; Wang et al., 2012; Sharma et al., 2019) has decreased significantly in the past 50 years associated especially in lakes with seasonally and inter-annually intermittent formation of ice (Franssen & Scherrer, 2008). Earlier ice breakup may lead to longer periods of water column stratification, warmer surface water temperature and increased heat storage in the lake during summer(O'Reilly, Alin, Plisnier, Cohen, & McKee, 2003; Livingstone, 2003; Mishra et al., 2011). Furthermore, a shorter duration of ice cover causes an extension of the stratified period and thus the growing season, which increases the probability of the development of anoxic conditions in deep waters at the end of the growing season (Livingstone, 1993). Assessment of the implications of global change, in particular climate warming, on hydrodynamics, primary production and water quality can be aided by numerical models that simulate ice-cover in temperate lakes with seasonal ice cover (Oveisy, Boegman, & Imberger, 2012). Furthermore, coupled hydrodynamic models that simulate spatial and temporal evolution of thin ice (< 10 cm thickness) are required to assess the climate warming impacts on the water column.

A wide variety of lake models has been developed to simulate hydrodynamics, thermal stratification and water quality in lakes. One-dimensional models are based on the assumption that horizontal gradients are negligible and that the vertical mixing can be described as a 1D process (Perroud, Goyette, Martynov, Beniston, & Annevillec, 2009;

Kirillin et al., 2011; Oveisy & Boegman, 2014b; Yao et al., 2014). These models have difficulty in describing deep vertical mixing mechanistically because boundary mixing, the dominant cause of vertical mixing in the hypolimnion (Goudsmit, Peeters, Gloor, & Wüest, 1997), and internal waves, the main sources of kinetic energy in deep waters, are inherently three dimensional processes (Goudsmit, Burchard, Peeters, & Wüest, 2002). In large lakes or those with complicated morphology, 3D hydrodynamic models can capture the spatial variability of physical and biogeochemical properties, and overcome the difficulties described above for 1D models. However, it is quite common to investigate the long-term trend of ice cover with 1D models (Fang & Stefan, 1996; Duguay et al., 2003; Dibike, Prowse, Bonsal, de Rham, & Saloranta, 2012; Yao et al., 2014)
because multi-year simulations with 3D models require a high computational time.

Application of 3D models to simulate multi-year conditions in mid-latitude, temperate lakes that freeze partially or completely need to consider ice formation (Oveisy, Rao, Leon, & Bocaniov, 2014a) to adequately reproduce not only winter conditions but also the seasonal changes in stratification after ice-off. 3D hydrodynamic models coupled with an ice formation module have the potential to simulate not only the development and thickness but also the temporal evolution of the spatial distribution of the ice cover in lakes.
One of the first applications of a three dimensional ice simulations used a four-layer model (atmosphere, snow, ice and ocean) to qualitatively simulate the spatio-temporal evolution of ice cover in Arctic and Antarctic lakes (Parkinson & Washington, 1979). More details of the ice-formation process were captured with the snow and ice version Dynamic Reservoir Simulation Model (DYRESM) by Patterson and Hamblin (1988), although the model was monodimensional. It incorporates a thermodynamic lake mixing model of the water column and it considered the 2-dimensional effect of partial ice cover. In Rogers et al. (1995) the Mixed Lake with Ice (MLI) cover model extended the DYRESM model, including new processes such as snowmelt due to rain, formation of white ice, and variability of snow density and albedo, specifically for mid-latitudes lakes. Oveisy et al. (2012) incorporated the ice-formation model of Rogers et al. (1995) in the 3D-hydrodynamic model Estuary and Lake Computer Model (ELCOM), extending its application to 3D ice-formation studies. This coupled model was validated by comparing model simulations with observations in a large lake (Ontario) and a small lake (Harmon, British Columbia, Canada) for one winter (Oveisy et al., 2012). Afterwards, Oveisy et al. (2014a) used the ice module coupled to ELCOM to investigate the effect of ice cover on the hydrodynamics and water quality in Lake Erie. ELCOM has recently been revised and renamed as the Aquatic Ecosystem Model, AEM3D (Hodges & Dallimore, 2018), which is based on the former model ELCOM, including the ice-formation module of Oveisy et al. 2012.
There are several other ice models coupled with 3D hydrodynamic model, for example the 3D ice-formation model used in Wang et al. (2010) and in Fujisaki et al. (2012). They both used the 3D Princeton Ocean Model (POM) coupled with the ice thermodynamic

formulation of Hibler (1979). This model allows for dynamic advection of ice but it is mostly used for coarse-resolution simulations in large systems (i.e. oceans, Great Lakes).

ELCOM has been used widely to represent the thermal structure and circulation patterns in many lakes (Leon, Antenucci, Rao, & McCrimmon, 2012) and has also been applied to address several research questions in the deepest basin of Lake Constance (Fig. 1), Upper Lake Constance, (Appt, Imberger, & Kobus, 2004; Eder, Rinke, Kempke, Huber, & Wolf, 2008; Lang, Schick, & Schroder, 2010; Dissanayake, Hofmann, & Peeters, 2019). But none of these studies focused on ice formation, cover and break-up, or on Lower Lake Constance (Fig. 1), the shallowest basin of Lake Constance, that experiences occasional ice cover in winter. The correct simulation of ice formation in this lake is an important requirement for further assessments of the implications of environmental changes on the system and to compare them with the response to the same forcing of the deeper neighboring system, Upper Lake Constance. The possibility to couple the hydrodynamic model ELCOM, together with its ice module, to a water quality model rendered it a suitable tool for further research applications to Lake Constance. Therefore, the understanding of the possible alterations of Lake Constance ecosystem due to environmental changes and the ecological, cultural, social and economic implications are relevant, since Lake Constance is a vital resource for human uses (bathing, irrigation, tourism, drinking water supply, winter recreation) and one of the most representative and important wetland habitat for plants and animals in Central Europe.

In this study we applied AEM3D to simulate nine consecutive years of water column thermal structure and the spatial distribution and temporal course of ice cover in the three basins of Lower Lake Constance (LLC). LLC is a temperate lake with a complex shape, subdivided into three basins. The ice information gathered from citizen reported data showed that the different basins do not necessarily freeze each year and are characterized by a large inter-annual and spatial variability of ice cover.
Model results are compared to observations of water temperature and ice cover in the three lake basins of LLC to test model performance with respect to the inter-annual occurrence of ice, the areal percentage of ice cover, the representation of differences in the occurrence and extent of ice cover, and the timing of ice formation and ice break-up. The objective of this study is to test whether AEM3D reproduces inter-annual variability and spatial heterogeneity of the thin ice cover that develops in a lake with complex morphology. Moreover, this work provides a unique example of ice model validation with data derived from a citizen science approach.

Methods

Study site

Lake Constance (9°18'E, 47°39'N) is an Alpine lake of glacial origin located in the southwest of Germany that conjointly borders Switzerland and Austria. Lake Constance (LC) consists of two main parts, Upper Lake Constance (ULC) and Lower Lake Constance (LLC), which are connected by the river Seerhein. ULC has a surface area of 473 km^2 and a maximum depth of about 251 m, whereas LLC is significantly smaller having a surface area of 63 km^2 and maximum and mean depth of 46 and 25 m, respectively. LLC is subdivided into three basins of different depths and hydro-geological features (Fig. 1). The southern part, where the river Seerhein enters, is called Rheinsee (RS). It is the deepest sub-basin of LLC and is influenced by the high discharge of the river Seerhein entering the sub-basin in the East and leaving it in the West. RS has a maximum depth of 24m and it is connected to Zeller See (ZS) in its northern part. This basin is strongly influenced by the exchange with RS and experiences large density-driven intrusions at intermediate depth due to the influence of the Seerhein. The second main inflow of LLC, Radolfzeller Aach, discharges into this sub-basin. The most northern sub-basin of LLC is Gnadensee (GS) having a maximum water depth of 20 m. GS is the most enclosed sub-basin without significant inflows. It is connected to ZS via a narrow and shallow sill (average water depth of about 2.5 m; Fig. 1), that limits the horizontal exchange of water to the two other basins.

In contrast to ULC, LLC develops regularly partial or complete ice cover during winter. According to Franssen and Scherrer (2008) complete or almost complete ice cover was observed 36 times in the last century but is less frequent nowadays. During the last decade, only in 2010, 2012 and 2017 ice cover developed in all the three sub-basins of LLC, resulting in almost full ice cover of the entire lake. However, full areal ice cover rarely develops in ZS and RS, while in GS it occurs much more frequently. The official documents from the Water Police of Constance did not describe the formation of ice cover thicker than 10 cm. The collected multimedia information showed that the undeformed ice is the dominating ice form in LLC but along the shores it is common to find brash ice or even pancake ice, formed by the action of wind on the water surface.

Model description

In order to simulate the lake hydrodynamic and thermal structure, we used the three dimensional model Hydrodynamic-Aquatic Ecosystem Model (AEM3D, Hodges & Dallimore, 2018). The hydrodynamic model, based on ELCOM, uses the unsteady Reynolds-averaged Navier-Stokes equations for heat and momentum and considers heat and momentum transfer across the water surface due to wind and atmospheric thermodynamics (Leon et al., 2011). The equations are solved numerically using a Cartesian Arakawa C-grid in the horizontal dimension and the vertical discretization is based on fixed Z-layers (Hodges, 2000). The equations are solved in all wet cells and a turbulent kinetic energy based mixed-layer model is used for vertical turbulent mixing. The model includes Earth rotation, wind

stress at the surface, surface thermal forcing, and inflows and outflows. More details can be found in Hodges (1998) and Hodges and Dallimore (2018).

The ice-formation algorithm described in Oveisy et al. (2012) was implemented in the model to simulate ice cover and its influence on lake hydrodynamics and thermal structure. Thus, multi-annual simulations can be performed for water bodies that experience regular ice cover. The ice-model is based on the formulation of Rogers et al. (1995) utilizing a one-dimensional steady-state equation of heat fluxes between ice, atmosphere and water column. The equations are applied independently in each grid cell, allowing spatially variable ice thickness and concentration due to spatially heterogeneous cooling and heat capacity of the surface mixed layer of the lake (Oveisy et al., 2012), without horizontal influence between the grid cells. The model cannot reproduce the horizontal transport of ice and ice deformation, since the advective transport is not modelled.

Model set up

AEM3D was set up for a continuous run from 4 March 2009 to 31 March 2018 based on the availability of meteorological input data and field observations. Because no data on water temperature of the main inflow of LLC, the river Seerhein, was available, the water temperature of the river Seerhein was derived from an independent hydrodynamic simulation of the entire LC (Suppl. B).

The computational grid of LLC was described by a regular, horizontal grid of 100 m x 100 m and 79 vertical layers, refined to 0.5 m near the surface and decreasing up to 1 m near the bottom. The two main inflows Seerhein and Radolfzeller Aach, and the outflow of river Rhein (Fig. 1) were set as boundary conditions by using the time series of measured discharge and water temperature. In case of Seerhein the water temperature was taken from the output of the simulation of LC. The outflow of LLC was derived from a water balance based on the inflows and the measured change in water level (gauge Berlingen). This approach corrected for discrepancies in the water balance arising from neglecting discharge of smaller tributaries and evaporation from the lake surface.

Water temperatures in LLC were initialized using temperature profiles measured with a CTD-probe (Conductivity, Temperature, Depth) at the stations M_{ZS}, M_{GS}, M_{RS}. The model internally interpolated water temperatures over the entire water volume using an inverse distance weighting method.

Spatially resolved wind fields were available for ULC (see below) and linearly interpolated to the computational grid. Except for the wind field, the model was driven with horizontally uniform meteorological data. Heat fluxes were calculated from air temperature, relative humidity, cloud cover and solar radiation. Longwave radiation was calculated in the model internally from an empirical relation from the Stefan-Boltzmann equation as a function of air temperature, cloud cover and relative humidity (Hodges, 1998).

A more detailed description of the model parametrization can be found in Suppl. B.

Data

Meteorological data

Hourly meteorological data on air temperature (Fig. 2), relative humidity, air pressure, cloud cover and solar radiation were available from the climate station in Konstanz maintained by the German National Meteorological Service (DWD: 47°40'390''N, 09°11'24''E; 442 m above sea level; Fig. 1). Spatially resolved wind fields were obtained from the numerical weather system of the Consortium for Small Scale Modeling (COSMO), which is operationally run at the National Swiss Weather Service (Doms & Baldauf, 2018). COSMO is a forecasting model to calculate future atmospheric conditions with a temporal output interval of 1 hour and a spatial resolution of 2.2 km (COSMO-2) and, since April 2016, 1.1 km (COSMO-1). The model COSMO-1 is initialized every hour with a field obtained by combining observation data, previous model runs and climatological information, in order to provide higher accuracy.

Inflow and outflow data

Daily or hourly river discharge data and river water temperature data were obtained from different sources: the Landesanstalt fuer Umwelt Baden-Wuerttemberg (LUBW), the Hydrographische Dienst Vorarlberg (VA), and the Federal Office for the Environment (BAFU). The latter also provided daily data on water level of LLC (gauge Berlingen).

Temperature data

Profiles of water temperature are available for station EU and FU in ULC and stations M_{GS}, M_{ZS}, and M_{RS} for LLC. At station EU, data are collected by a thermistor chain with a vertical resolution from 0.5 to 2 m in the upper mixed layer (down to 20 m depth) and a coarser vertical resolution in the hypolimnion. From regular monitoring programs by the IGKB (the International Commission for water protection of Lake Constance) and LUBW, CTD profiles are available for the stations M_{ZS} and M_{GS} and less resolved data at station M_{RS} and FU (resolution 2.5 – 5 m and 5 – 20 m respectively).

Ice data

Data on ice cover have been rarely recorded for Alpine lakes that do not freeze regularly (Franssen & Scherrer, 2008). For LLC, no continuous and systematic records on ice cover exist. However, Franssen and Scherrer (2008) reconstructed the ice history of LLC in the 20th century, combining sporadic records by the Water Police and information from local newspapers. We extended this time series on ice cover by collecting all available information on ice data, e.g., reports of the Water Police, local newspapers, news blogs, and social media for the winters between the years 2010 and 2018. The collected data set was employed to define when ice was abundant and in which lake basins.

The most valuable sources of information on ice cover were from reports of the Water Police. These reports provide a qualitative description of the ice cover pattern for specific dates, mentioning if the frozen areas were safe or not to bear the load of people. This information from the police reports was complemented with information from newspaper articles (Südkurier Online, St. Gallen Tagblatt), descriptions on blogs and pictures or videos from people spending time on the ice that were posted on social media (Instagram, YouTube). Especially for recent winters, such as in 2017 and 2018, ice data from social media were an important source of information. These data can be assumed as useful information to define the timing of ice-on and -off and whether it is thick enough to bear the load of people.

An additional source of information, especially for the year 2011, were reports of the LUBW which mentioned in their field protocols the accessibility of the different monitoring stations in the three sub-basins of LLC. A detailed list of the sources and the collected data is provided in Suppl. A. In some years, we could not find any information in any report or in the media about ice cover the sub-basins of LLC. In such cases, we assumed that no significant ice cover in the specific lake basin was formed.

We checked whether satellite images could provide additional information on the occurrence of ice and the spatial distribution of ice cover. But most of the time obscuring effects due to cloud cover and fog typical for LLC during wintertime as well as difficulties in distinguishing blue ice from water prevent obtaining better information on ice than evaluated from the ground truth data.

Ice data was interpreted with respect to the reference scale of the US Army Corps of Engineers (CRREL-US Army Corps of Engineers). They defined ice ≥5 cm as safe ice, thick enough to bear the load of a single person per square meter. Hence, the distinction made by the Water Police between safe and dangerous frozen areas was interpreted in the same way: the frozen areas stated as safe in the ice reports provide information on the presence of ice with a thickness ≥5 cm, while dangerous frozen areas refer to thinner ice. Pictures or videos with only a few people on ice were referred to thinner ice (~3 cm) in case they were taken before the Water Police mentioned safe ice. The available data do not provide information on very thin ice (<3 cm), because it is too dangerous to attract people to walk on it and thus unlikely to find pictures of people on the ice. Further, the Water Police typically does not report on very thin ice.

The onset of observed ice cover, $ONSET_{obs}$, was defined as the date of the first observation of ice cover within the respective winter. This information was always a picture showing people on the ice along the shores, where ice typically starts to freeze and thus safer than further offshore. These pictures at $ONSET_{obs}$ were always taken before the Water Police reported safe ice. Hence, ice thickness at $ONSET_{obs}$ was assumed to be ~3 cm in accordance to the interpretation of the ice data described above.

The onset of modelled ice cover $ONSET_{sim}$ was defined as the date at which the simulated mean ice thickness over the ice area was thicker than 3 cm and covered at least 10% of the

surface area of the basin. $ONSET_{sim}$ was evaluated separately for each basin for the winters 2017 and 2018, when the most frequent ice data was available.

Analysis of the air temperature data

Air temperature is a key parameter that relates to the formation and break-up of ice (Franssen & Scherrer, 2008). A derived parameter often used for this purpose is the sum of Negative Degree Days (NDD) that discriminates very cold winters from mild ones. The sum of NDD was computed from the time series of the daily mean air temperature according to Franssen and Scherrer (2008) during the period 1 October to 31 March for each of the simulated winters (Fig. 2). In the same study, Franssen and Scherrer (2008) defined that for Lower Lake Constance the sum of NDD for which the lake freezes with a probability of 10, 33, 50, 67 and 90% are respectively 128, 156, 170, 187 and 228°C·days, respectively. The sum of NDD corresponding to a probability of 10% (128°C·days) was used to discriminate between cold and mild winters.

Model validation: simulated thermal structure

At stations M_{GS} and M_{ZS} the results of the model simulations were compared to temperature profiles focusing on different stratification regimes of three consecutive years (2010, 2011, 2012): mixed or inversely-stratified at the beginning for December - March; initially stratified in April - May; stratified in June - September; stratified before the overturn in October-November.

The accuracy of the simulated thermal structure was evaluated using the root mean square error (RMSE) between each temperature profile and the output of the model at the same date t_j:

$$RMSE(t_j) = \left[\frac{1}{N}\sum_{i=1}^{N}(x_i(t_j) - y_i(t_j))^2\right]^{1/2} \quad (1)$$

where x_i and y_i are the measured and simulated temperatures at the date t_j, respectively. Both model and data were interpolated to a vertical grid of 0.1 m, where i=1,..,*N* represents the number of points in the vertical profile. The RMSE of each of the four periods was computed as the average RMSE of the profiles in each period.

The accuracy of the water temperature simulation in winter was computed as the RMSE between the modeled temperature at 1 m depth, y_s, and the temperature observations at 1 m depth, x_s:

$$RMSE_{surface} = \left[\frac{1}{M}\sum_{j=1}^{M}(x_s(t_j) - y_s(t_j))^2\right]^{1/2} \quad (2)$$

where *M* is the number of temperature profiles collected in the winter 2010, 2011 and 2012.

Model validation: simulated ice cover

Simulated lake ice cover was validated with the available observations between the winter 2010 (W2010) and 2018 (W2018; Fig. 4). We used the notation WYYYY to designate the time period from 1 December of the previous year to 30 April of the named year YYYY. Although the lack of detailed records documenting the ice timing, the sourced validation data provided a very useful avenue for qualitative information on the abundance of ice cover.
The model output consists of a time series on the spatial distribution of ice thickness in LLC. The simulated ice thickness was subdivided into four classes: 1 - 3 cm, 3 - 5 cm, 5 - 7 cm and ≥ 7 cm. Then, the simulated percentage of the lake area covered by ice of a specific thickness class was computed as the ratio between the number of ice covered surface cells of the considered class and the overall number of surface cells. In addition to the surface fraction covered by ice of different thickness, ice volume was calculated as well.
The simulated ice cover was compared to observations of the different lake basins separately (Fig. 5). The amount of ice in each basin was expressed as the specific volume of ice cover (cm), which was defined as the ratio between the simulated ice volume in each basin and the corresponding surface area. This allows a comparison of the volume of ice between basins with different surface area.
A detailed comparison between model and observation on the spatial distribution of ice coverage and thickness in LLC was conducted for three different dates in W2017 (21, 26 and 29 January), because for these dates the reports from the Water Police were particularly detailed.

Results

Long-term simulation of thermal structure

Lower Lake Constance (LLC) shows stable stratification during the summer and inverse stratification during the winter months, and further, can be considered as dimictic showing complete mixing during autumn overturn as well as in spring after ice-off. According to the model output, inverse stratification develops 10-15 days before the occurrence of ice cover and it is established in the top 1-2 m below the ice (Suppl. B). The inverse stratification disappears due to vertical convective mixing during ice-off.

Model results and observations were compared at two sites (M_{GS} and M_{ZS}) and for three consecutive years (2010, 2011, and 2012) to validate the model performance in terms of thermal structure throughout the season and among years (Fig. 3). The simulated temperature profiles during ice-free periods in winter adequately represented conditions observed in the water column, while the simulated temperatures during the stratified period deviated more from observations.

The agreement between simulated thermal structure and monthly temperature profiles was evaluated using the root mean square error (RMSE). A mean RMSE was computed for each of the four periods described above (December-March; April-May; June-September; October-November) and is presented in Tab. 1. The model represents the thermal structure most accurately between October and March, with a mean RMSE between 0.37 and 1.08°C in ZS and 0.97 and 1.82°C in GS. During the winter months (from December to March), the mean RMSE was 0.85, 0.37, 0.45 °C in ZS for the years 2010, 2011, 2012 and 1.03, 0.98 °C in GS for the years 2010, 2012 (no data available in 2011). The simulation was least accurate in the period June to September, with a maximum mean RMSE of 1.49 in M_{ZS} and 2.34°C in M_{GS}. In each case, the model reproduced the thermal structure more accurately at station M_{ZS} than M_{GS}. In the period December to March, the $RMSE_{surface}$ at 1 m depth was 0.80°C and 0.89°C in M_{ZS}.

Inter-annual variability of ice cover

Between 2010 and 2018, winters ranged from cold to mild, causing a wide range of ice coverage and duration. W2010 and W2012 can be regarded as cold winters with NDD ≥128°C·days. The other winters were characterized by a smaller sum of NDD and can be then considered as mild winters, in particular W2014, W2015 and W2016 with a sum of NDD <40°C·days (Fig. 2). During the simulated decade, abundant ice cover was observed in W2010, W2011, W2012 and W2017. Less ice cover was observed in W2016 and W2018, during which significant ice cover only developed in GS. For the remaining years, no information was documented, suggesting no or at most very little and intermittent ice cover.

The pattern of ice occurrence simulated with AEM3D agrees rather well with the observed pattern (Fig. 4). The simulated ice coverage of LLC showed a marked inter-annual variability. In the years when abundant ice cover was observed, the model results showed the largest

extent of ice, with up to 80-90% coverage of the lake surface. In W2014 and W2016, an ice thickness >5 cm did not form or covered <20% of the lake surface area.
Ice coverage does not contain information on ice thickness and ice cover can be misleading with respect the amount of ice formed. For example, in W2015 a large percentage of the ice cover was thin, with only 13% of the ice cover of thickness ≥5 cm. While the percentage of lake ice coverage in W2015 was similar to that in W2011, the corresponding simulated ice volume was only half with respect to W2015. The pattern of inter-annual variability in simulated ice volume agrees very well with observations of the abundance of ice cover: the four years for which abundant ice was reported correspond with the largest simulated ice volumes (Fig. 3b).

Inter-basin variability of ice cover

The observations indicate that ice formation and spatial coverage developed differently between the three basins of LLC. Almost complete ice cover regularly develops on GS, which is documented by abundant observations. In contrast to GS, ZS and RS have much less ice cover and the ice forms only infrequently. GS was almost fully ice covered in W2010, W2011, W2012, and W2017, partially frozen in W2018, and barely frozen in areas along the shores in W2016. Ice cover in ZS was observed in W2010, W2012 and W2017, while it was ice free in W2018. Very small ice covered areas were reported in RS in W2012 and W2017, but not in the other years.
Consistent with the data, the model simulation showed a significant difference in occurrence and specific volume of ice among the basins (Fig. 5). In the model, a thick ice cover developed in GS almost every winter, except for the W2015 and W2016, when only thin ice was formed. In contrast to GS, ZS was ice covered in the model only in W2010, W2011, W2012 and W2017, and RS developed only thin ice in these years. The model also captured the absence of ice in RS in W2016 and W2018. Furthermore, the model always reproduced thicker ice in GS than in the other basins. Ice ≥5 cm occurred in GS in all winters except in W2014 and W2016. In ZS, ice ≥5 cm was less frequent than in GS and occurred in the W2010, W2011, and W2017. In contrast, in RS ice ≥5 cm was almost never formed, except at very low percentage area in W2010 and W2011. Hence, the simulated specific ice volume was always highest in GS and decreased from GS over ZS to RS (Fig. 4b).
A quantitative measure to compare the extent and duration of ice cover between the different sub-basins was defined by counting the number of days during which ice cover exceeds 50% and 80% of the basin surface area. GS showed the highest number of days above these thresholds (Tab. 2): 50% of the basin surface area was ice covered every year for 8 to 87 days and 80% of the basin surface area was covered in all winters except in W2014 and W2016. When ice cover was >80% of the basin surface area, it lasted between 28 and 85 days.
Ice cover in the other two sub-basins was less extensive (Tab. 2). In ZS ice coverage >50% of the surface area occurred for more than half of the winters (W2010, W2011, W2012, W2015 and W2017) and lasted between 21 and 79 days. Periods of ice cover in ZS that

exceeded 50%, also exceeded 80%, but for a shorter period, i.e. 10 to 60 days. In RS, 50% of ice cover occurred in the same years as in ZS, and as well in W2013 for7 days. Ice coverage >80% occurred only in W2012 for 8 days. In RS ice was typically formed for shorter periods than in the two other lake basins.

Simulated and measured ice cover distributions in the sub-basins were investigated in more detail for two consecutive winters (W2017 and W2018). For these two winters the most detailed information on ice cover were available but the meteorological conditions differed substantially between these years (Figs. 2 and 6). Moreover, the spatial distribution of ice cover and the timing of ice-on and ice-off differed substantially between the two winters. W2017 was characterized by a long, cold period in January, with almost four consecutive weeks of negative daily mean air temperature and 92°C·days negative degree days between October and March (Fig. 2). Ice cover formed in all three sub-basins of the lake. In GS ice records were documented for the entire month of January and February, but only at the end of January in the other two basins. Instead, in W2018 continuous negative daily mean air temperature was recorded for 11 days between 20 February and 2 March and in total 52.3°C·days negative degree days between October and March (Fig. 2). In this winter, only GS froze over between the end of February and the first week of March (documented by observations).

The model reproduced well the ice that formed in all three basins in W2017 and only in GS in W2018. In W2017 ice cover reached 100% in GS, with a maximum specific volume (ratio between the simulated ice volume of the basin and its surface area) of >4 cm from 26 January to 28 February and a maximum specific volume of 5.6 cm (Fig. 6). In W2018 the ice cover reached almost 100%, but the specific volume >4 cm was present only for a short period (29 February to 5 March) and the maximum specific volume was more than 1 cm smaller than in W2017. In W2017 the model reproduced ice cover in the other two basins too, but the ice volume was considerable smaller: the maximum specific volume was 3.8 cm and 2.5 cm in ZS and RS, respectively.

In GS, the first observation of ice cover ($ONSET_{obs}$) was on 6 January in W2017 and on the 25 February in W2018. The simulated onset of ice cover ($ONSET_{sim}$) was on the 16 January in W2017and on the 25 February in W2018. In GS, $ONSET_{sim}$ was later in W2017 and agreed very well in W2018 with $ONSET_{obs}$. In the other basins, $ONSET_{obs}$ was on 17 January in ZS and on 23 January in RS in W2017, whereas $ONSET_{sim}$ was on 29 January in ZS and 3 February in RS.

The simulated ice cover was compared qualitatively to the pattern of ice cover derived from the report of the Water Police (Fig. 7) in order to validate model results regarding the spatial distribution of ice, ice coverage and timing of ice-on and -off. From the description of the reports, the first dangerous frozen areas (<5 cm) were distributed along the shore of GS on 21 January 2017. A safe frozen area (≥5cm) was observed in the southern part of the basin at this time. After 5 days, the ice around the shore of GS became thicker and extended toward offshore up to 300 m. During that time, the center of the basin was covered by thin ice, regarded as not safe by the Water Police. At the same time, ice started to develop along

the shores of ZS and RS. On 29 January, the safe frozen areas along the shores of GS become wider (up to 400 m) and the frozen area in the south enlarged. At this time, the center of the basin was completely covered by ice, but was still regarded as dangerous in the reports. On the last day analyzed, ice cover along the shores of ZS and RS had extended and thickened. The model simulation showed a predominance of ice between 3 and 5 cm in the basin of GS on 21 January (Fig. 7). Ice ≥5 cm thick was found in a small area in the southern part of Gnadensee, while the center of the basin was characterized by ice with thickness between 1 and 3 cm. On 26 January, the ice in GS became thicker and reached ≥7 cm in the southern part of the lake. Ice between 3 and 5 cm also extended along the shores of ZS and RS and a layer of thin ice covered this basin completely and almost half of RS. On 29 January, GS was almost covered by ice with a thickness ≥5 cm, beside the area of the sill between GS and ZS. 3-5 cm thick ice was present along the shores of ZS and RS, as well as an extended layer of thin ice.

Discussion

Ice data

In many studies investigating the spatial distribution of ice, model results have been validated against ice-cover information derived from satellite images. Ground truth data were available in Fujisaki et al. (2013), but not in the studies by Oveisy et al. (2012) and Oveisy et al. (2014a). In LLC, cloud cover and fog are typical features during wintertime, limiting the applicability of commonly used satellite imagery for ice detection. In addition, the differentiation between ice covered areas and open water was not possible, presumably due to the presence of thin black ice without snow cover. The use of multi-sourced data to validate an ice modelling study is an interesting alternative to a remote sensing approach to collect ice data that rendered this work unique in the field of 3D ice modelling.

Model simulations vs. observations

a) Considerations of the thermal structure

We first investigated the ability of the model to reproduce the seasonal thermal structure of the lake and the surface water temperature, with particular attention to the winter months. The vertical thermal structure during ice-free winters was well reproduced by the model, as indicated by a maximum mean RMSE of only 1.0°C, which is similar to the error obtained in Oveisy et al. (2012). Specifically, the RMSE of the surface water temperature in the ice-free winters was 0.89°C in ZS and 0.80°C in GS. In Oveisy et al. (2014a) the comparison of simulated temperatures with the satellite-derived lake surface temperatures showed a similar deviation (RMSE=0.87°C).

The RMSE obtained in summer periods were larger than in winter because during stratified periods the exact vertical position of the thermocline is difficult to simulate, which is a known challenge. In general, the model showed a tendency to reproduce a deeper thermocline than observations and this deviation was largest in GS, the most enclosed sub-basin. Multi-annual simulation in Lake Erie showed similar deviations between modelled and observed thermocline depth (Fujisaki et al., 2013).

According to the model in the top 1-2 m of the water column, a weak inverse stratification is established during wintertime (Suppl. B). The development of inverse stratification starts up to 10-15 days before the formation of ice cover and it disappears during ice-off. Since the sampling interval of the regular monitoring was comparatively large, the probability capturing periods of inverse stratification before ice cover occurs is low, and measurements from the ice are typically not conducted because of safety reasons.

b) Considerations of the simulation of ice cover

The model demonstrated its sensitivity to the annual variability of climate in reproducing the occurrence of ice in LLC: in W2014, W2015, W2016 and W2018 simulated ice extents were small, whereas they were large in W2010, W2011, W2012 and W2017, which is in accordance with the observations (Fig. 3).

The model differentiated frequent and abundant occurrence of ice in GS from less frequent and less abundant ice cover in the other two sub-basins. The simulation results showed that GS was fully covered almost every year, while the other basins were ice-free or characterized by only partial ice cover and thinner ice. Hence, the resulting simulated specific ice volume was always larger in GS than in the other basins. Moreover, the simulated ice cover lasted longer and occurred more often in winters in GS than in the other basins (Tab. 2).

The onset of freezing was in reasonable accordance with observations (Fig. 6): in W2017 the simulated $ONSET_{sim}$ in GS occurred about 10 days later than $ONSET_{obs}$, while in W2018 $ONSET_{sim}$ coincided with $ONSET_{obs}$. Also in the other two basins, $ONSET_{sim}$ gave reasonable description of the freezing time in W2017 and W2018. The frequently collected data for these two winters allowed a detailed comparison between the simulated and observed timing of ice cover that was not possible in previous studies using the same ice module. For example, in the model application to Lake Erie by Oveisy et al. (2014a) the comparison between data and simulations is based on monthly observations the first of which already indicates a full ice cover with a lake-wide average ice thickness of about 4 cm. In the study of Yao et al. (2014) comparing the application of four different 1D models for multi-years ice simulations, the deviation between data and model on the timing of ice-on and-off was up to 20 days, thus larger than in our study. The model agreement with the ice data for multi-years simulations resulted to be even more difficult with a 3D model, like in Fujisaki et al. (2013), where the deviations model-data for some years were off of about 30 days.

The model results in the study here not only agreed reasonably well with the observed onset of freezing but also represented well the differences in the spatial ice extent in the three sub-basins at specific dates. The spatial coverage of simulated ice ≥5 cm replicated the frozen area classified as safe by the Water Police, while the dangerous frozen areas overlap with the pattern of the simulated ice with a thickness between 3 and 5 cm. The simulations show also the development of thin ice <3 cm, which is typically formed during the onset of ice. Without modeling the process of thin ice break-up by surface waves, the model is likely to simulate an earlier onset of very thin ice cover (Oveisy et al., 2014a). Additionally, the lack of advective ice dynamics in the ice-formation model limits the description of the deformed ice, that can develop along the shores of LLC. Nevertheless, these consequences will be less pronounced in lakes with limited fetch (e.g. in small lakes) and consequently smaller surface waves and thus will lead to better model representation of ice cover and duration in small compared to large lakes.

Application of 3-D hydrodynamic models to simulate multi-year changes in ice cover are rare (e.g. Fujisaki et al. 2013). Previous studies applying the model AEM3D to ice covered lakes have considered only single winters (Oveisy et al., 2012; Oveisy et al., 2014a), but did not include continuous multi-year simulations.

Applications of 3D hydrodynamic models to ice cover development and ice cover distribution have focused mainly on large lakes, e.g. Lake Ontario (Oveisy et al., 2012) or Lake Erie (Fujisaki et al., 2013; Oveisy et al., 2014a). The only application of a coupled 3D

hydrodynamic - ice model to a small lake was conducted on Lake Harmon (Oveisy et al., 2012). However, the latter study focused on the increase and decline in ice thickness above 10 cm but did not consider the development and melt away of ice nor ice cover with a thickness below 10 cm. In general, previous 3D studies have typically not investigated ice formation in lakes where ice thickness remains below 10 cm during the entire winter season, as it is common in LLC and many other medium-sized to small, temperate lakes. In the study on Lake Erie by Fujisaki et al. (2013) observed ice cover was up to 50 cm thick and most of the observations available referred to ice thickness >10 cm. In the cases when ice thickness was <10 cm the agreement between model and observations was rather low: the model simulated up to 30 cm of ice, even where there was no ice cover (Fujisaki et al., 2013).

The study here applying the coupled 3D hydrodynamic-ice model AEM3D to LLC simulating ice cover development and ice cover distribution continuously over several years in a sub-divided lake that partially freezes and typically develops thin ice cover with thickness below 10 cm extends the range of 3D model applications to ice cover simulation in lakes. The model results demonstrate that comparatively thin ice with thickness below 10 cm can be simulated reasonably well and that differences in ice cover between adjacent basins in a lake with complex morphometry can also be captured well by the model. The results also show that inter-annual variability of partial and spatially heterogeneous ice cover in LLC is captured well by the model.

Conclusion

The 3D hydrodynamic model AEM3D coupled with an ice module allows seasonally resolved as well as multi-year simulations of water temperature and ice cover and in temperate lakes. The application of the model to LLC, a lake consisting of three distinct but connected basins with hydrodynamically different conditions showed a good agreement between the simulated and observed inter-annual variation in the spatial distribution of ice cover, ice thickness and duration of ice cover. The ice formation and extent differed gradually between the three sub-basins. In temperate lakes, inter-annually variable and partial ice formation is a common feature, and the adequate simulation of such conditions requires reliable reproduction of thin ice with thickness below 10 cm.

The results suggest that the 3D hydrodynamic model AEM3D with its ice module is a powerful tool cover in lakes or reservoirs with partially and inter-annually variable ice. It can be useful to reconstruct the history of ice in lakes lacking spatiotemporal ice records or to forecast ice formation, distribution and thickness under future scenarios, e.g. climate change. In this respect, the application of 3D models can help to understand the impact of climate warming on partially and intermittent ice covered lakes regarding hydrodynamic conditions and water quality, e.g. phytoplankton growth and oxygen.

Data availability statement

The ice data that support this finding are available in the supplement A, while the rest of the data is available from the corresponding author upon reasonable request.

References

Appt, J., Imberger, J., & Kobus, H. (2004). Basin-scale motion in stratified Upper Lake Constance. *Limnology and Oceanography*, *49*(4), 919–933.

Arrigo, K. R., Perovich, D. K., Pickart, R. S., Brown, Z. W., Van Dijken, G. L., Lowry, K. E., … Bahr, F. (2012). Massive phytoplankton blooms under Arctic sea ice. *Science*, *336*(6087), 1408.

Austin, J., & Colman, S. (2008). A century of temperature variability in Lake Superior. *Limnology and Oceanography*, *53*(6), 2724–2730.

CRREL-US Army Corps of Engineers. Web site: http://www.integralhse.co.uk/ice-safety/

Dessai, S., Hulme, M., Lempert, R., & Pielke Jr, R. (2009). Climate prediction: a limit to adaptation. *Adapting to Climate Change: Thresholds, Values, Governance*, 64–78.

Dibike, Y., Prowse, T., Bonsal, B., de Rham, L., & Saloranta, T. (2012). Simulation of North American lake-ice cover characteristics under contemporary and future climate conditions. *International Journal of Climatology*, *32*(5), 695–709.

Dissanayake, P., Hofmann, H. and F. Peeters (2019). Comparison of results from two 3D hydrodynamic models with field data: internal seiches and horizontal currents. *Inland waters*. https://doi.org/10.1080/20442041.2019.1580079

Doms, G., Baldauf, M., & Baldauf, M. (2018). Consortium for Small-Scale Modelling A Description of the Nonhydrostatic Regional COSMO-Model Part I : Dynamics and Numerics.

Duguay, C. R., Flato, G. M., Jeffries, M. O., Ménard, P., Morris, K., & Rouse, W. R. (2003). Ice-cover variability on shallow lakes at high latitudes: model simulations and observations. *Hydrological Processes*, *17*(17), 3465–3483.

Eder, M., Rinke, K., Kempke, S., Huber, A., & Wolf, T. (2008). Seeweite Bodensee-Messkampagne 2007 als Test für BodenseeOnline. *WasserWirtschaft*, *98*(10), 34–38.

Fang, X., & Stefan, H. G. (1996). Long-term lake water temperature and ice cover simulations/measurements. *Cold Regions Science and Technology*, *24*(3), 289–304.

Franssen, H. J. H., & Scherrer. (2008). Freezing of lakes on the Swiss plateau in the period 1901-2006. *International Journal for Climatology*, *28*(December 2008). https://doi.org/10.1002/joc

Fujisaki, A., Wang, J., Hu, H., Schwab, D. J., Hawley, N., & Rao, Y. R. (2012). A modeling study of ice–water processes for Lake Erie applying coupled ice-circulation models. *Journal of Great Lakes Research*, *38*(4), 585–599.

Fujisaki, A., Wang, J., Bai, X., Leshkevich, G., & Lofgren, B. (2013). Model-simulated interannual variability of Lake Erie ice cover, circulation, and thermal structure in

response to atmospheric forcing, 2003–2012. *Journal of Geophysical Research: Oceans*, *118*(9), 4286–4304.

Gerbush, M. R., Kristovich, D. A. R., & Laird, N. F. (2008). Mesoscale boundary layer and heat flux variations over pack ice–covered Lake Erie. *Journal of Applied Meteorology and Climatology*, *47*(2), 668–682.

Goudsmit, G., Peeters, F., Gloor, M., & Wüest, A. (1997). Boundary versus internal diapycnal mixing in stratified natural waters. *Journal of Geophysical Research: Oceans*, *102*(C13), 27903–27914.

Goudsmit, G., Burchard, H., Peeters, F., & Wüest, A. (2002). Application of k-ϵ turbulence models to enclosed basins: The role of internal seiches. *Journal of Geophysical Research: Oceans*, *107*(C12).

Hamilton, D. P., Magee, M. R., Wu, C. H., & Kratz, T. K. (2018). Ice cover and thermal regime in a dimictic seepage lake under climate change. *Inland Waters*, *8*(3), 381–398.

Hampton, S. E., Galloway, A. W. E., Powers, S. M., Ozersky, T., Woo, K. H., Batt, R. D., … Lottig, N. R. (2017). Ecology under lake ice. *Ecology Letters*, *20*(1), 98–111.

Hibler, W. D. (1979). A dynamic thermodynamic sea ice model. *Journal of Physical Oceanography*, *9*(4), 815–846.

Hodges, B. (1998). Heat budget and thermodynamics at a free surface: Some theory and numerical implementation. *Centre for Water Research, University of Western Australia, Crawley, WA, Australia*.

Hodges, B. R. (2000). Numerical Techniques in CWR-ELCOM (code release v. 1). *CWR Manuscript WP*, *1422*.

Hodges, B., & Dallimore, C. (2018). HydroNumerics.

Hodgkins, G. A., James, I. C., & Huntington, T. G. (2002). Historical changes in lake ice-out dates as indicators of climate change in New England, 1850–2000. *International Journal of Climatology: A Journal of the Royal Meteorological Society*, *22*(15), 1819–1827.

Kirillin, G., Hochschild, J., Mironov, D., Terzhevik, A., Golosov, S., & Nützmann, G. (2011). FLake-Global: Online lake model with worldwide coverage. *Environmental Modelling & Software*, *26*(5), 683–684.

Lang, U., Schick, R., & Schroder, G. (2010). The decision support system Bodenseeonline for hydrodynamics and water quality in Lake Constance. In *Decision support systems, advances in*. IntechOpen.

Leon, L. F., Smith, R. E. H., Hipsey, M. R., Bocaniov, S. A., Higgins, S. N., Hecky, R. E., … Guildford, S. J. (2011). Application of a 3D hydrodynamic–biological model for seasonal and spatial dynamics of water quality and phytoplankton in Lake Erie. *Journal of Great Lakes Research*, *37*(1), 41–53.

Leon, L. F., Antenucci, J. P., Rao, Y. R., & McCrimmon, C. (2012). Summary performance of the Estuary and Lake Computer Model (ELCOM): application in the Laurentian and other Great Lakes. *Water Quality Research Journal*, *47*(3–4), 252–267.

Livingstone, D. M. (1993). Temporal structure in the deep-water temperature of four swiss lakes: A short-term climatic change indicator? *Internationale Vereinigung Für Theoretische Und Angewandte Limnologie: Verhandlungen*, *25*(1), 75–81.

Livingstone, D. M. (2003). Impact of secular climate change on the thermal structure of a large temperate central European lake. *Climatic Change*, *57*(1–2), 205–225.

Lizotte, M. P., Sharp, T. R., & Priscu, J. C. (1996). Phytoplankton dynamics in the stratified water column of Lake Bonney, Antarctica. *Polar Biology*, *16*(3), 155–162.

Loose, B., McGillis, W. R., Schlosser, P., Perovich, D., & Takahashi, T. (2009). Effects of freezing, growth, and ice cover on gas transport processes in laboratory seawater experiments. *Geophysical Research Letters*, *36*(5).

Magnuson, J. J., Robertson, D. M., Benson, B. J., Wynne, R. H., Livingstone, D. M., Arai, T., … Kuusisto, E. (2000). Historical trends in lake and river ice cover in the Northern Hemisphere. *Science*, *289*(5485), 1743–1746.

Mishra, V., Cherkauer, K. A., & Bowling, L. C. (2011). Changing thermal dynamics of lakes in the Great Lakes region: Role of ice cover feedbacks. *Global and Planetary Change*, *75*(3–4), 155–172.

O'Reilly, C. M., Alin, S. R., Plisnier, P.-D., Cohen, A. S., & McKee, B. A. (2003). Climate change decreases aquatic ecosystem productivity of Lake Tanganyika, Africa. *Nature*, *424*(6950), 766.

Okubo, A. (1971). Oceanic diffusion diagrams. In *Deep sea research and oceanographic abstracts* (Vol. 18, pp. 789–802). Elsevier.

Oveisy, A., Boegman, L., & Imberger, J. (2012). Three-dimensional simulation of lake and ice dynamics during winter. *Limnology and Oceanography*, *57*(1), 43–57.

Oveisy, A., Rao, Y. R., Leon, L. F., & Bocaniov, S. A. (2014a). Three-dimensional winter modeling and the effects of ice cover on hydrodynamics, thermal structure and water quality in Lake Erie. *Journal of Great Lakes Research*, *40*, 19–28.

Oveisy, A., & Boegman, L. (2014b). One-dimensional simulation of lake and ice dynamics during winter. *Journal of Limnology*, *73*(3).

Parkinson, C. L., & Washington, W. M. (1979). A large-scale numerical model of sea ice. *Journal of Geophysical Research: Oceans*, *84*(C1), 311–337.

Patterson, J. C., & Hamblin, P. F. (1988). Thermal simulation of a lake with winter ice cover 1. *Limnology and Oceanography*, *33*(3), 323–338.

Peeters, F., & Hofmann, H. (2015). Length-scale dependence of horizontal dispersion in the surface water of lakes, 1917–1934. https://doi.org/10.1002/lno.10141

Perroud, M., Goyette, S., Martynov, A., Beniston, M., & Annevillec, O. (2009). Simulation of multiannual thermal profiles in deep Lake Geneva: A comparison of one-dimensional lake models. *Limnology and Oceanography*, *54*(5), 1574–1594.

Rogers, C. K., Lawrence, G. A., & Hamblin, P. F. (1995). Observations and numericzal simulation of a shallow, *40*(March 1992), 374–385.

Sharma, S., Blagrave, K., Magnuson, J. J., O'Reilly, C. M., Oliver, S., Batt, R. D., … Winslow, L. (2019). Widespread loss of lake ice around the Northern Hemisphere in a warming world. *Nature Climate Change*, *9*(3), 227.

Stewart, K. M. (1988). TRACING INFLOWS IN A PHYSICAL MODEL OF LAKE CONSTANCE. *Journal of Great Lakes Research*, *14*(4), 466–478. https://doi.org/10.1016/S0380-1330(88)71579-8

Tilzer (1983). The importance of fractional light absorption by photosynthetic pigments for phytoplankton productivity in Lake Constance, *28*, 833–846.

Vanderploeg, H. A., Bolsenga, S. J., Fahnenstiel, G. L., Liebig, J. R., & Gardner, W. S. (1992). Plankton ecology in an ice-covered bay of Lake Michigan: Utilization of a winter phytoplankton bloom by reproducing copepods. *Hydrobiologia*, *243*(1), 175–183.

Wang, J., Hu, H., Schwab, D., Leshkevich, G., Beletsky, D., Hawley, N., & Clites, A. (2010). Development of the Great Lakes ice-circulation model (GLIM): application to Lake Erie in 2003–2004. *Journal of Great Lakes Research*, *36*(3), 425–436.

Wang, J., Bai, X., Hu, H., Clites, A., Colton, M., & Lofgren, B. (2012). Temporal and spatial variability of Great Lakes ice cover, 1973–2010. *Journal of Climate*, *25*(4), 1318–1329.

Weyhenmeyer, G. A., Westöö, A.-K., & Willén, E. (2007). Increasingly ice-free winters and their effects on water quality in Sweden's largest lakes. In *European Large Lakes Ecosystem changes and their ecological and socioeconomic impacts*. *Springer*, 111-118Yao, H., Samal, N. R., Joehnk, K. D., Fang, X., Bruce, L. C., Pierson, D. C., … James, A. (2014). Comparing ice and temperature simulations by four dynamic lake models in Harp Lake: past performance and future predictions. *Hydrological Processes*, *28*(16), 4587–4601.

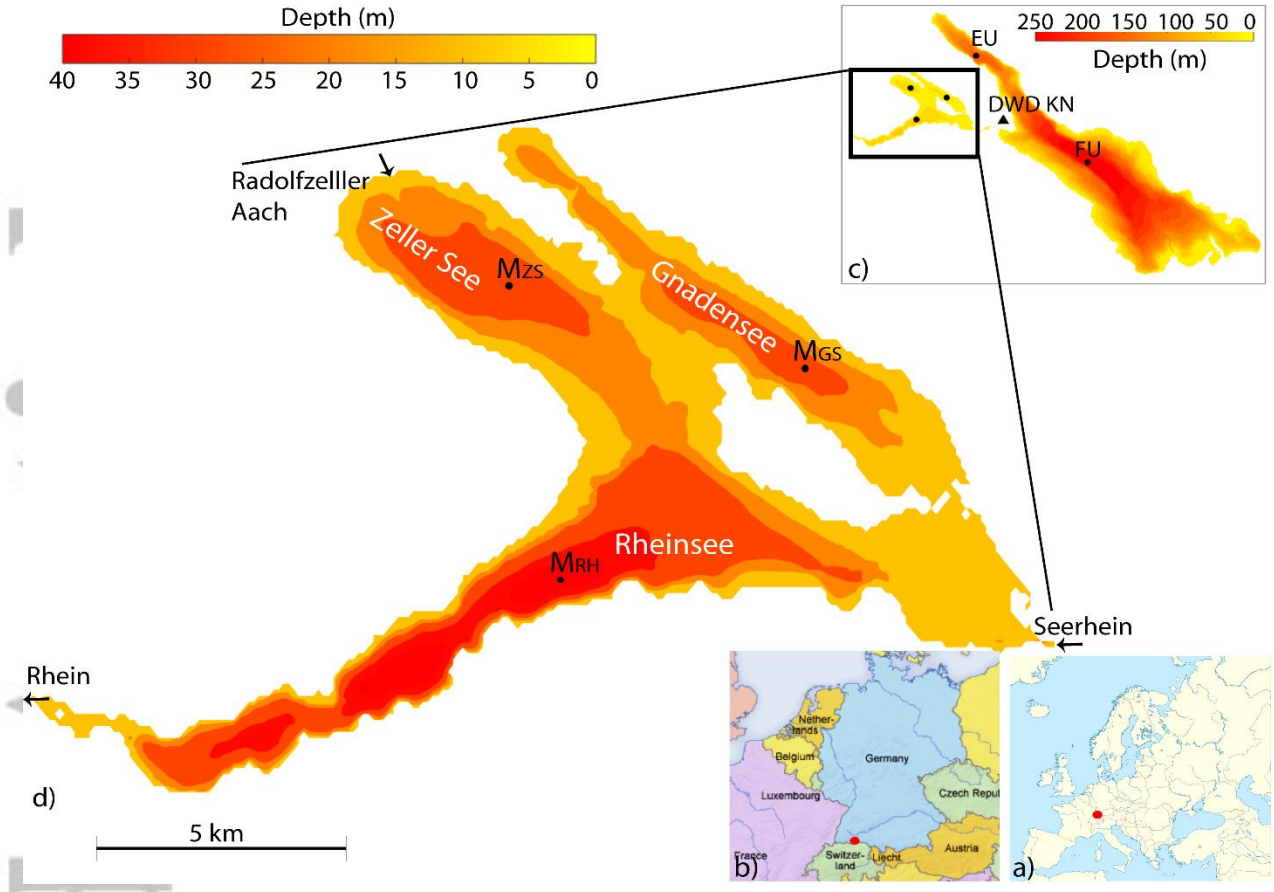

Figure 1: Bathymetry of the study site. a) and b) Location of Lake Constance in Europe. c) Bathymetry of Lake Constance and location of the meteorological station (DWD KN) and the stations used to initialize the model applied to LC. b) Bathymetry of Lower Lake Constance, distinguishing between the sub-basins and showing the main inflows and the outflow. Monitoring stations, used to initialize the model applied to LLC, were shown: M_{GS} is in the basin of Gnadensee, M_{ZS} in Zeller See and MRS in Rheinsee.

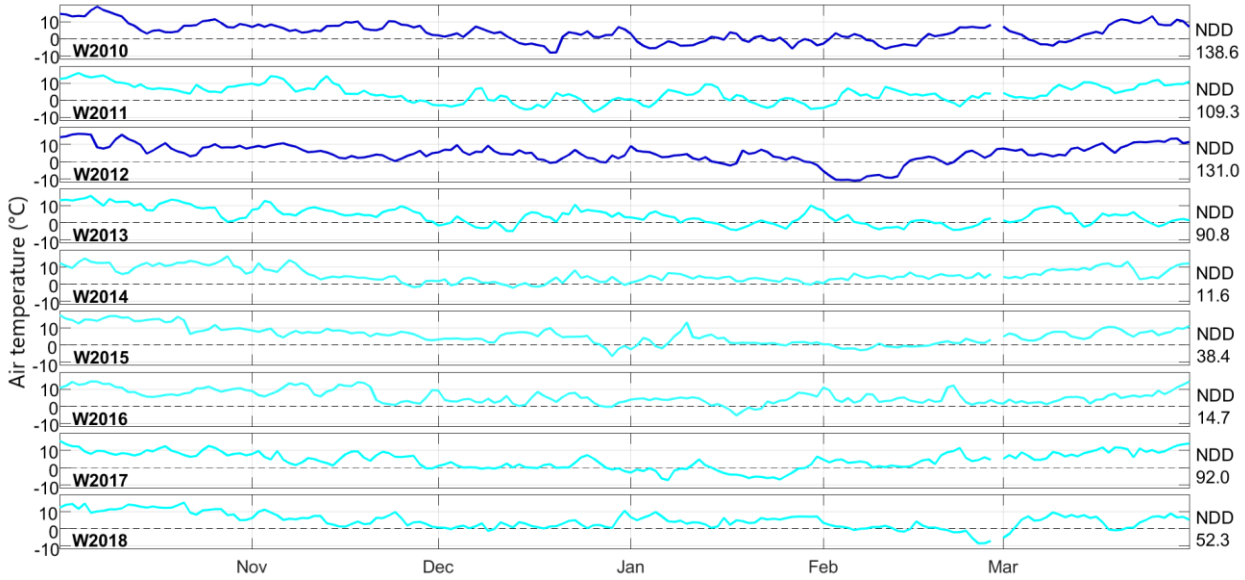

Figure 2: Time series of the air temperature at the DWD-station Konstanz between 1 October and 31 March for each of the simulated years. The sum of negative degree days (NDD in °C·days) is indicated on the right hand side of each panel. The color coding classified winters in two categories according to the sum of NDD: NDD <128 as mild winters and NDD ≥128 as cold winters.

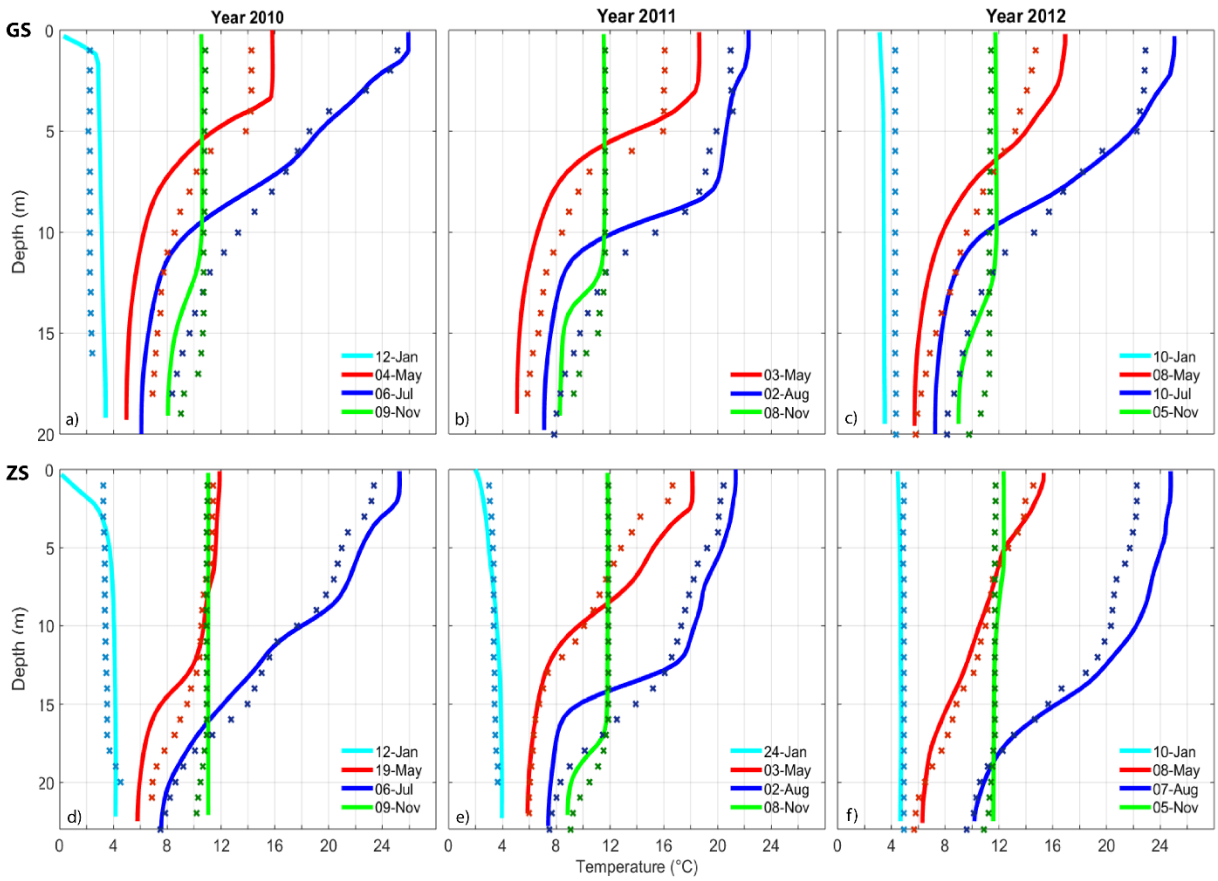

Figure 3: Seasonal differences in thermal structure and model validation. Comparison of observed (continuous line) and simulated (dotted line) temperature in Gnadensee (GS) and Zeller See (ZS) for characteristic snapshots (thermal structure) of three consecutive years (2010, 2011 and 2012).

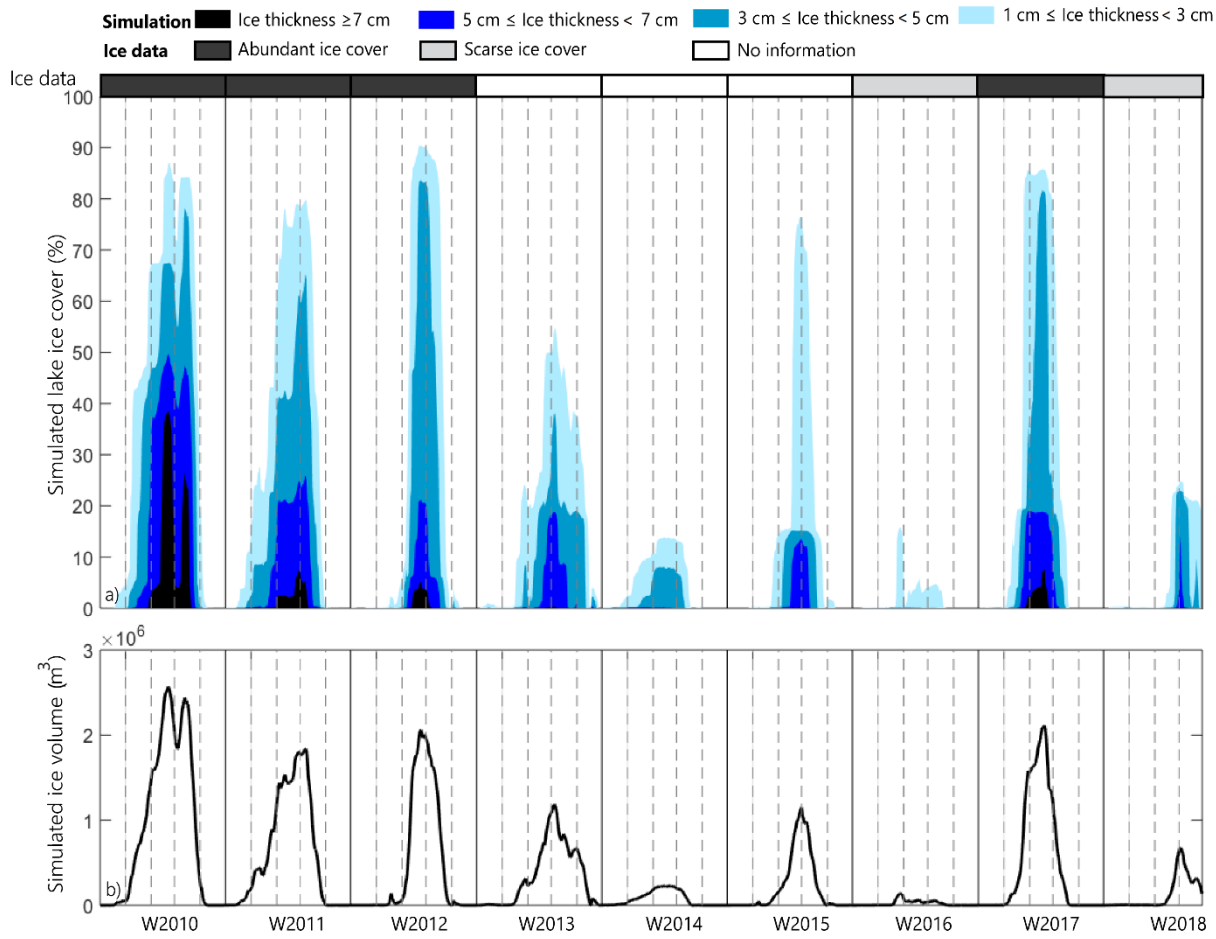

Figure 4: Annual variability of ice cover in Lower Lake Constance (LLC) in the period 2010 – 2018. a) Simulated lake ice cover percentage, distinguishing between four categories of ice thickness, compared to observed ice data. b) Time series of the simulated ice volume in LLC.

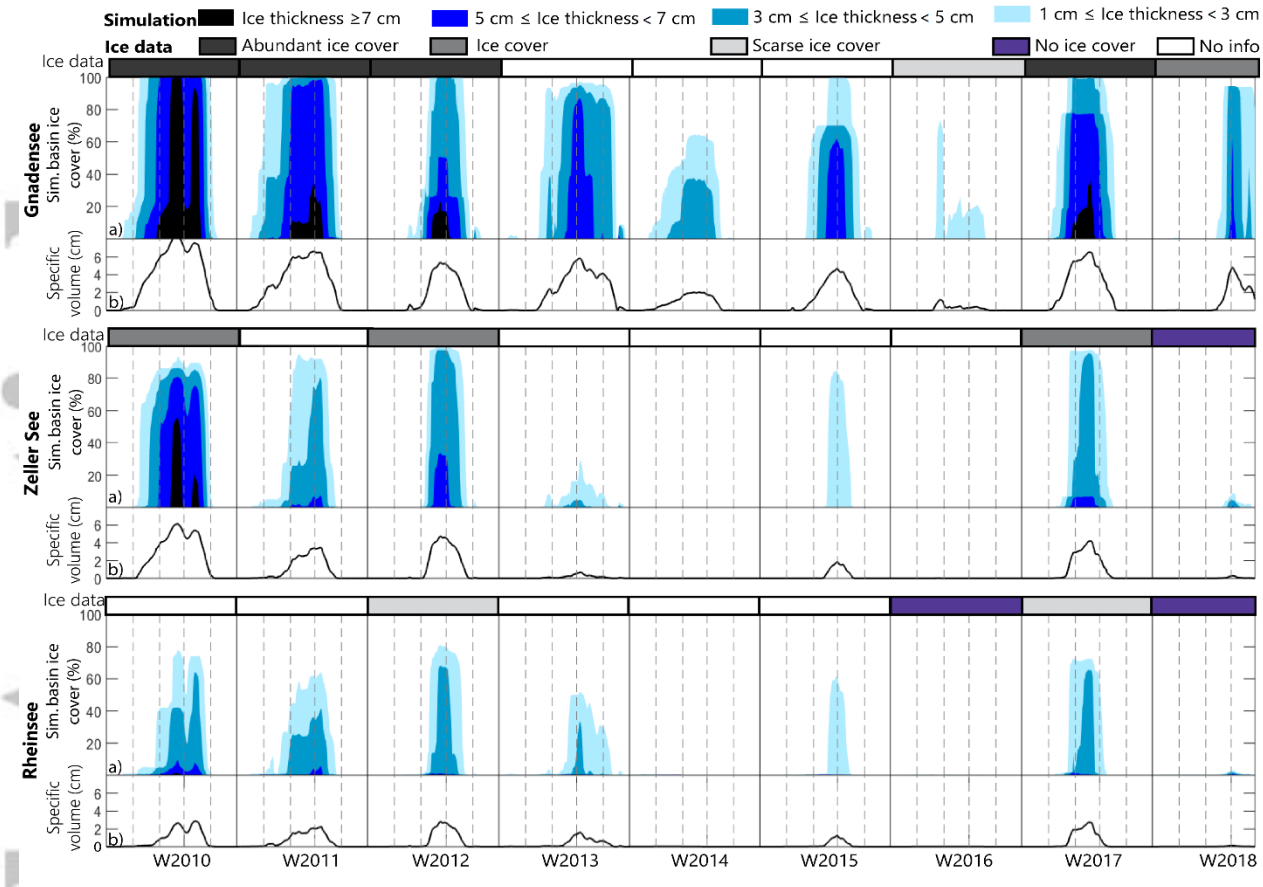

Figure 5: Inter-basin and annual variability of ice cover during the observation period (2010-2018). a) Comparison between simulated ice cover (%), distinguishing between four categories of ice thickness, and observed ice data for each of the basins. b) Specific volume given by the ratio between the simulated ice volume and the corresponding surface area of the basin.

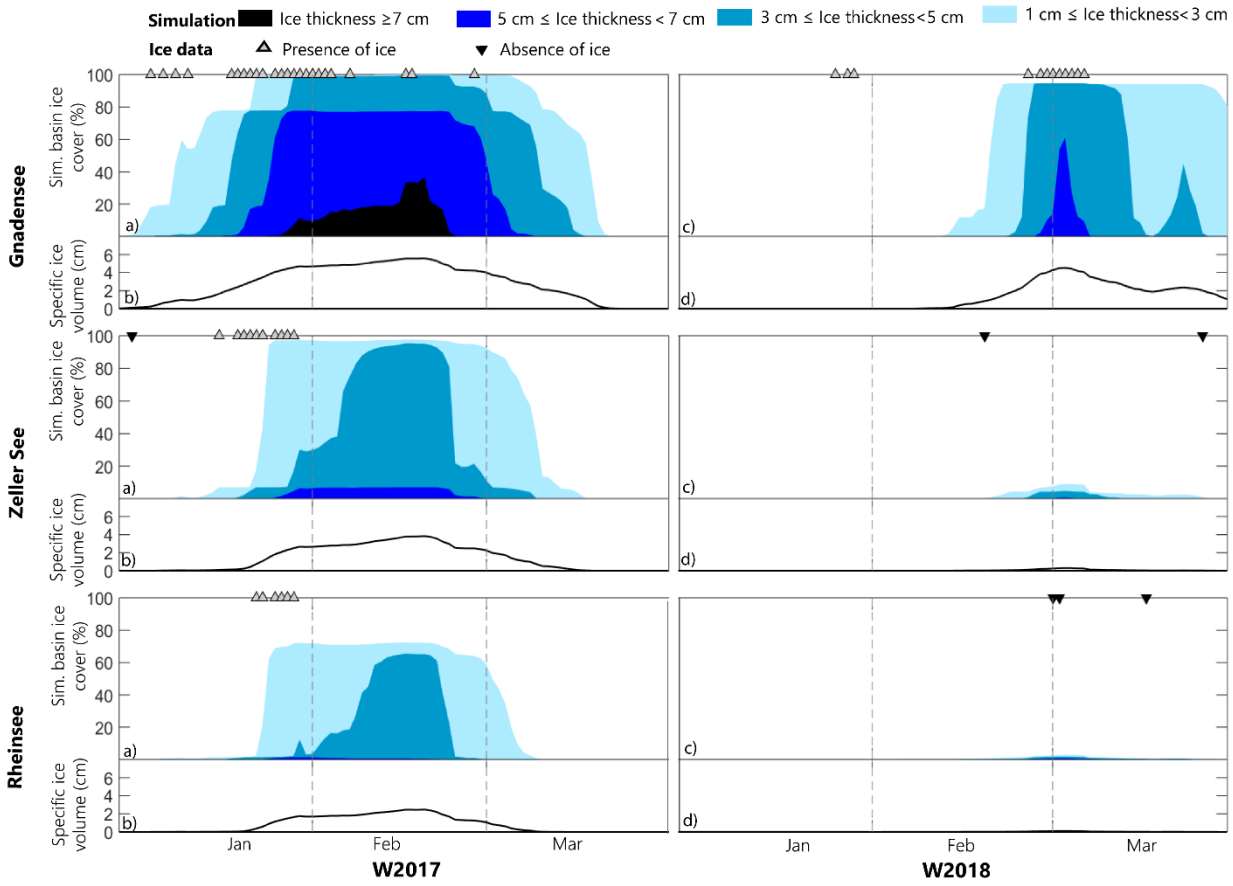

Figure 6: Inter-basin variability of ice cover in winter 2017 and 2018. a) Simulated ice cover (%) in Gnadensee (GS), Zeller See (ZS) and Rheinsee (RS) distinguishing between four categories of ice thickness, versus ice data. b) Specific ice volume given by the ratio between the simulated ice volume and the corresponding surface area of the specific basin.

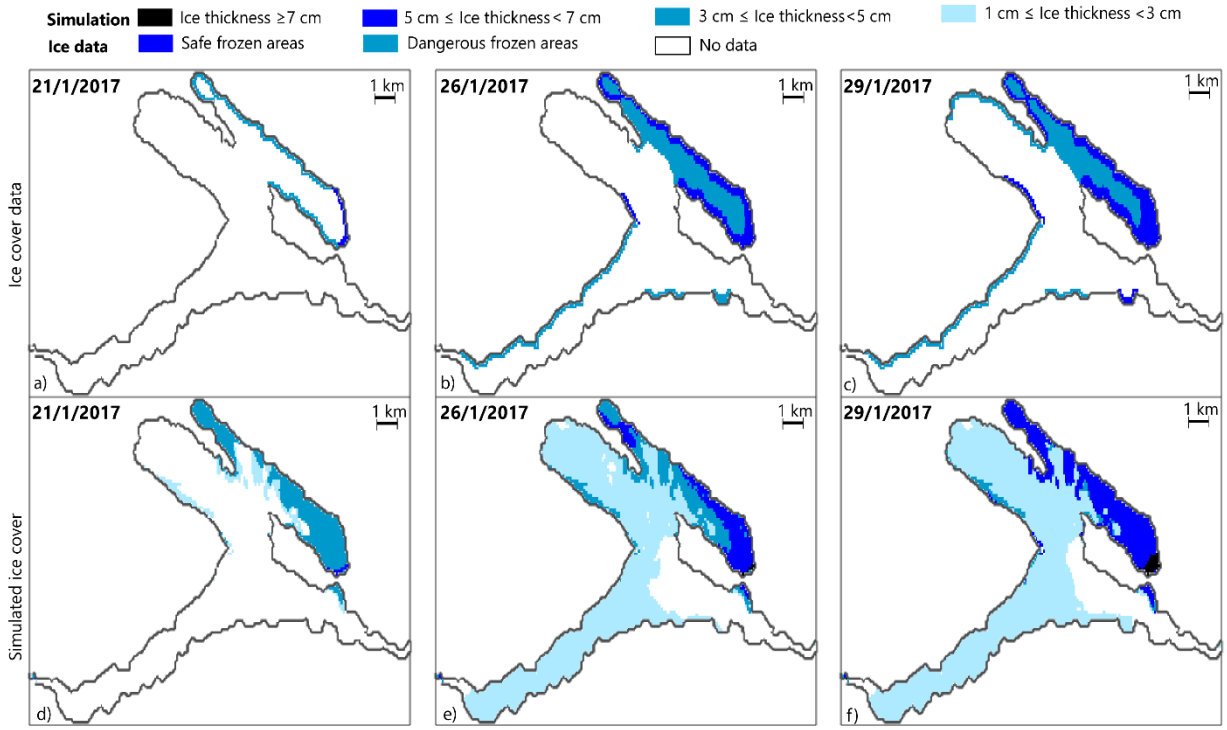

Figure 7: Detailed comparison of observed and simulated spatial distribution of ice cover for three days during the formation of ice (21st, 26th and 29th of January 2017).

Table 1: Model validation based on temperature. RMSE between measured and simulated temperature profiles of the sub-basins Gnadensee and Zeller See.

Gnadensee				
RMSE (°C)	Dec. - March	April - May	June – Sept.	Oct. – Nov.
2010	1.03	2.16	2.26	1.03
2011	-	2.01	2.06	1.82
2012	0.98	1.59	2.34	0.97
Zeller See				
RMSE (°C)	Dec. - March	April - May	June – Sept.	Oct. – Nov.
2010	0.85	1.12	1.32	1.02
2011	0.37	0.97	2.22	1.08
2012	0.45	0.51	1.49	0.35

Table 2: Number of days during which ice cover exceeds 50% and 80% of the basin surface area. The dash indicates winters that did not exceed the threshold. GS = Gnadensee, ZS = Zeller See and RS = Rheinsee.

(days)	GS >80%	ZS >80%	RS >80%	GS >50%	ZS >50%	RS >50%
W2010	85	60	-	87	79	37
W2011	82	40	-	85	46	35
W2012	41	39	8	47	44	37
W2013	80	-	-	82	-	7
W2014	-	-	-	33	-	-
W2015	28	10	-	57	21	15
W2016	-	-	-	8	-	-
W2017	46	39	-	66	43	36
W2018	38	-	-	39	-	-